Supplement of Atmos. Chem. Phys., 20, 15537–15549, 2020
https://doi.org/10.5194/acp-20-15537-2020-supplement

Atmospheric Chemistry and Physics
Open Access
EGU

Supplement of

Optical source apportionment and radiative effect of light-absorbing carbonaceous aerosols in a tropical marine monsoon climate zone: the importance of ship emissions

Qiyuan Wang et al.

Correspondence to: Qiyuan Wang (wangqy@ieecas.cn) and Junji Cao (cao@loess.llqg.ac.cn)

Table S1. Summary of aerosol light absorption from primary emissions ($Abs_{pri}(\lambda)$) and secondary formation ($Abs_{sec}(\lambda)$) during the campaign. λ represents the wavelength of 370, 470, 520, 590, 660, or 880 nm.

Type	Light absorption (Mm^{-1})	Standard deviation (Mm^{-1})	Absorption fraction (%)
$Abs_{pri}(370)$	14.9	8.6	95
$Abs_{sec}(370)$	0.8	1.8	5
$Abs_{pri}(470)$	10.8	5.7	96
$Abs_{sec}(470)$	0.5	0.9	4
$Abs_{pri}(520)$	9.1	4.7	96
$Abs_{sec}(520)$	0.4	0.7	4
$Abs_{pri}(590)$	7.8	4	96
$Abs_{sec}(590)$	0.3	0.6	4
$Abs_{pri}(660)$	6.6	3.3	97
$Abs_{sec}(660)$	0.2	0.4	3

Table S2. Results of bootstrap analysis.

	Motor vehicle emissions	Ship emissions	Fugitive dust	Biomass burning	Unmapped
Motor vehicle emissions	50	0	0	0	0
Ship emissions	0	49	1	0	0
Fugitive dust	0	1	49	0	0
Biomass burning	0	0	3	47	0

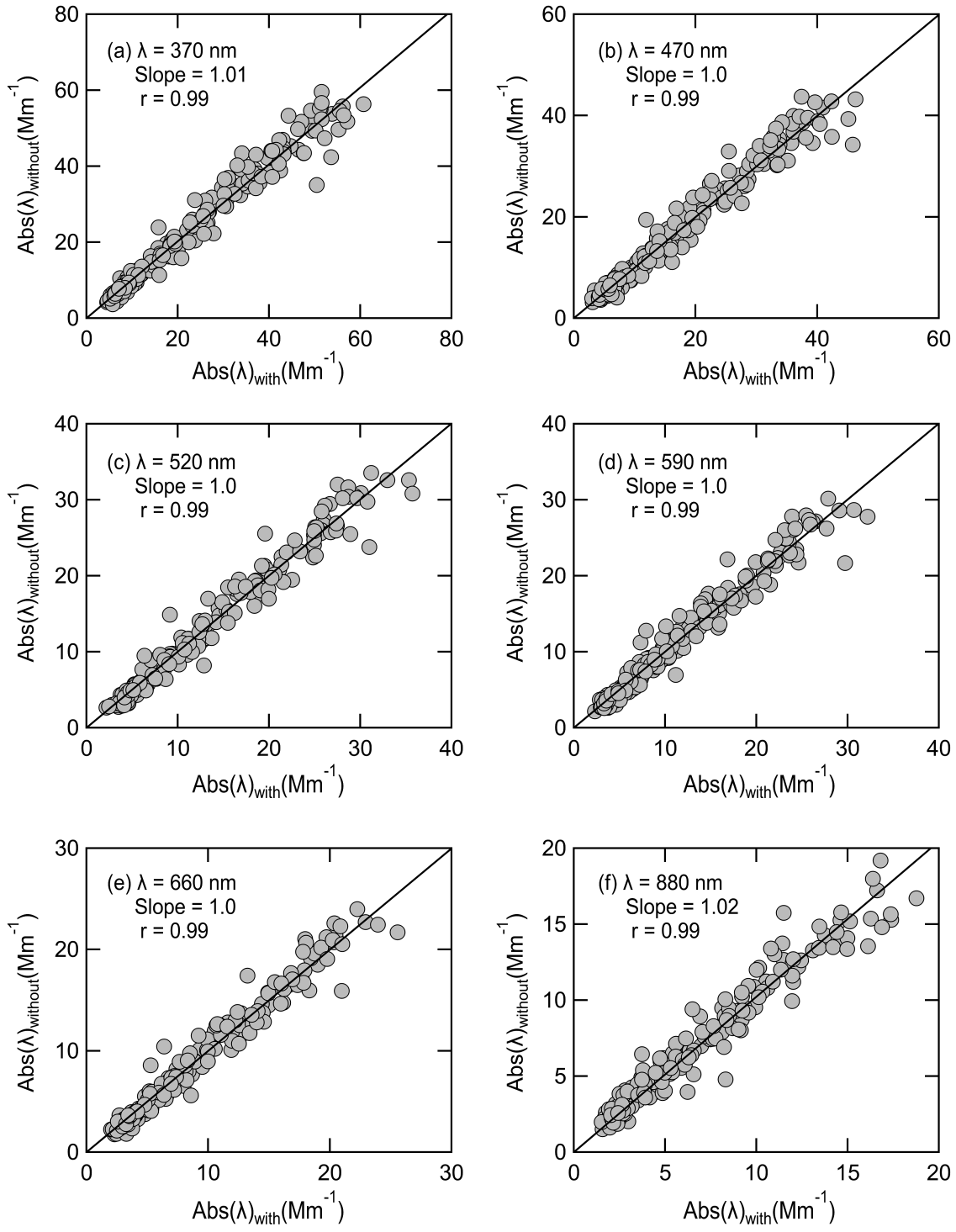

Figure S1. Scatter plots of light absorption coefficients measured with ($Abs(\lambda)_{with}$) and without ($Abs(\lambda)_{without}$) Nafion dryer (MD-700-24S-3). λ is the wavelength of 370, 470, 520, 590, 660, or 880 nm.

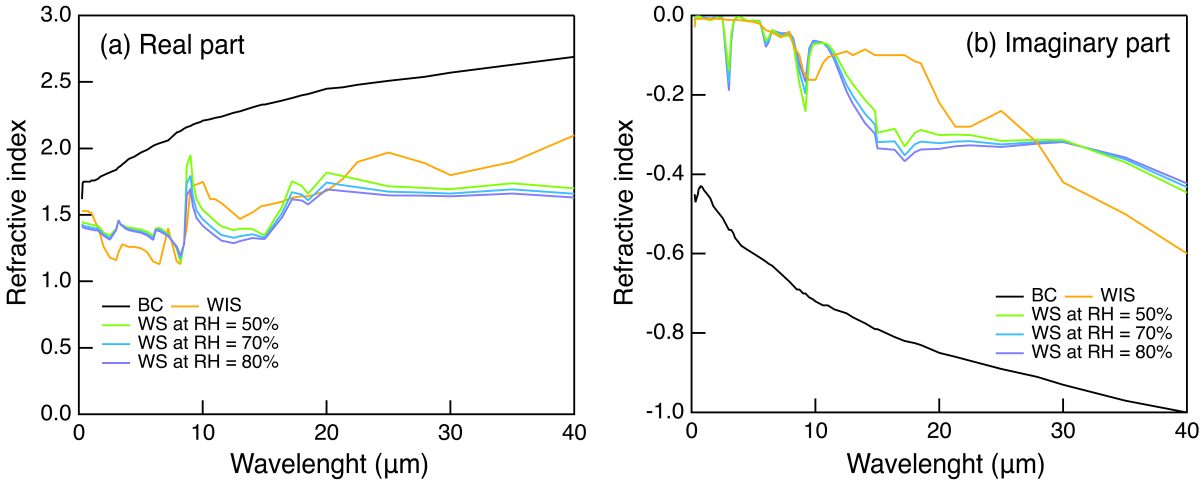

Figure S2. The refractive index (real part and imaginary part) of black carbon (BC), water-soluble (WS) components at different relative humidity (RH), and water-insoluble (WIS) components used in the Optical Properties of Aerosols and Clouds (OPAC) model.

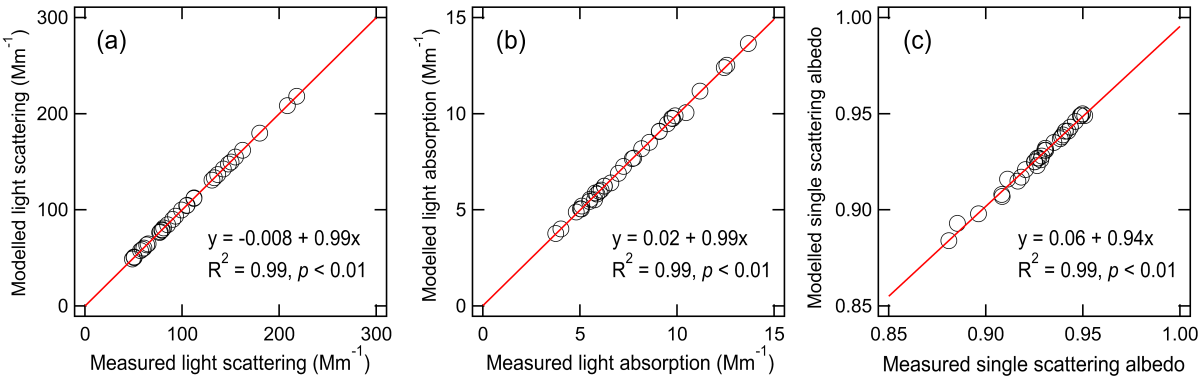

Figure S3. Scatter plots of optical parameters modelled with Optical Properties of Aerosol and Cloud model versus values measured with a photoacoustic extinctiometer.

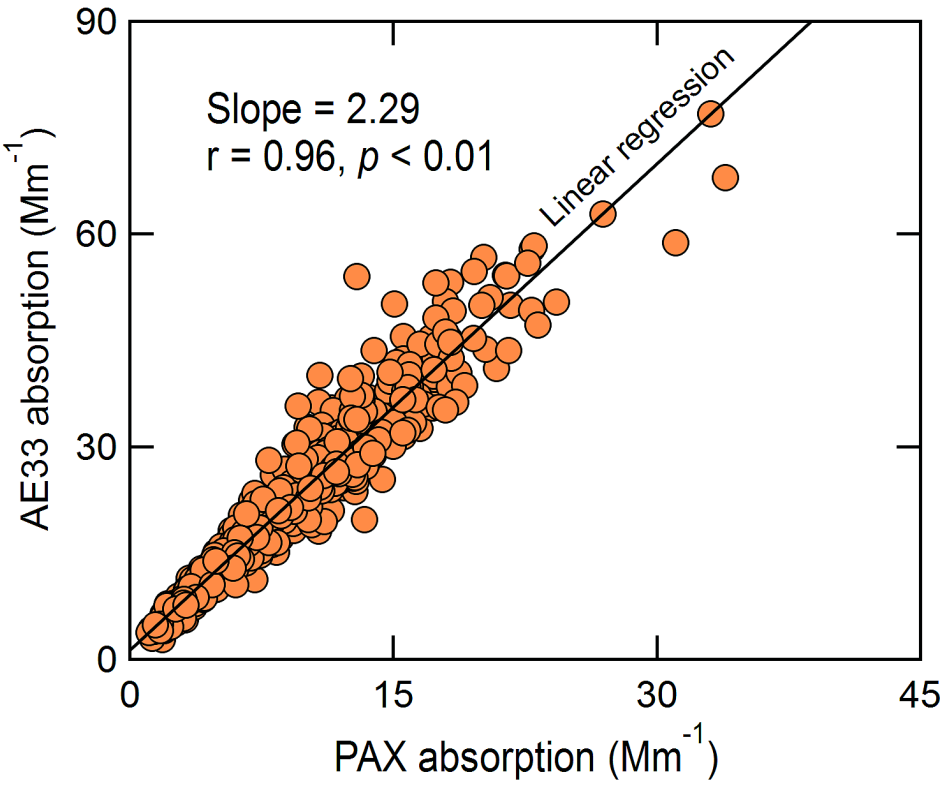

Figure S4. Relationship between the light absorption coefficient measured using a model AE33 aethalometer at wavelength of 520 nm and a photoacoustic extinctiometer (PAX) at wavelength of 532 nm.

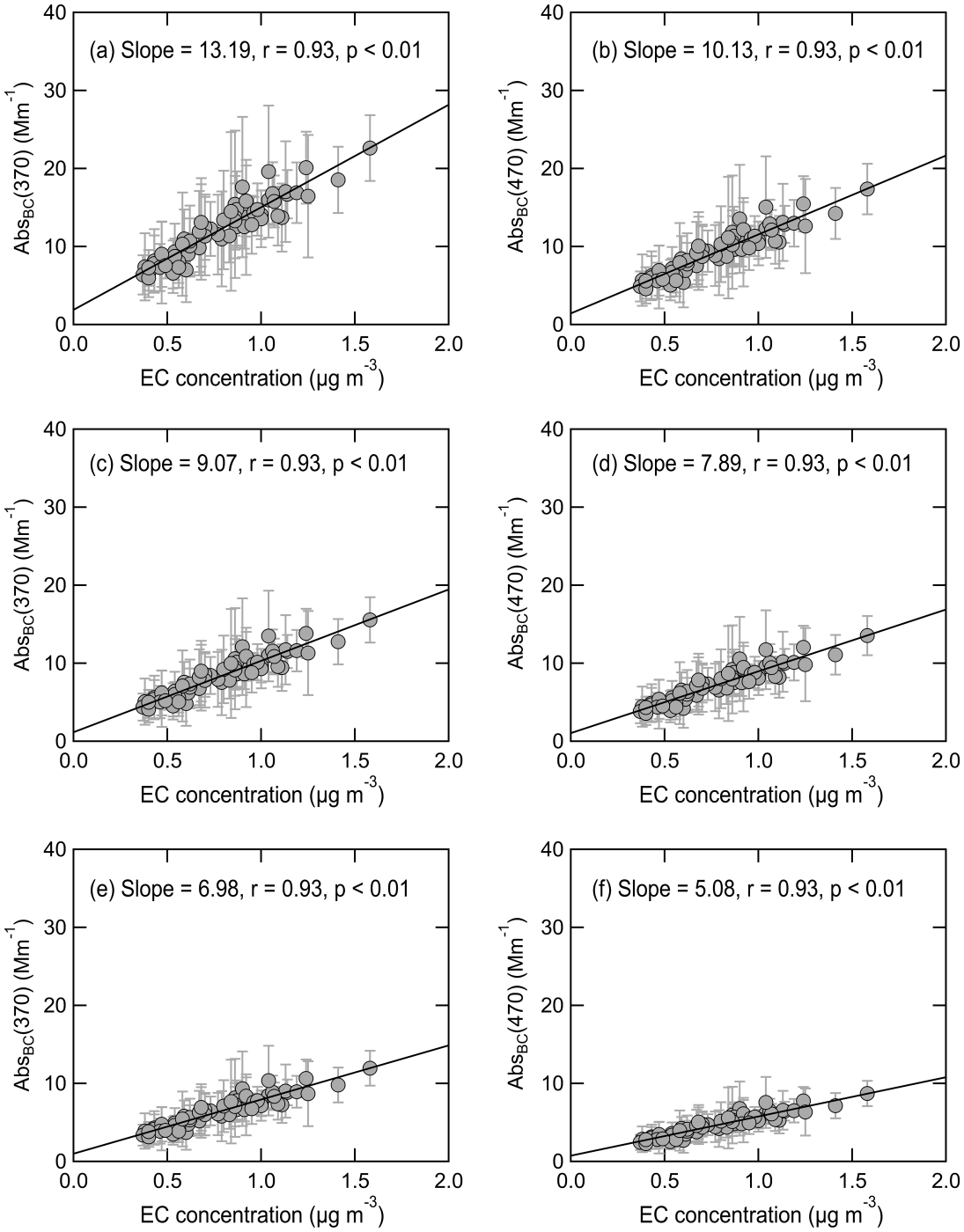

Figure S5. Scatter plots of light absorption of black carbon at different wavelengths ($Abs_{BC}(\lambda)$, λ = 370, 470, 520, 590, 660, and 880 nm) versus mass concentration of elemental carbon (EC). The black lines are the linear regression. The vertical error bars represent one standard deviation of $Abs_{BC}(\lambda)$.

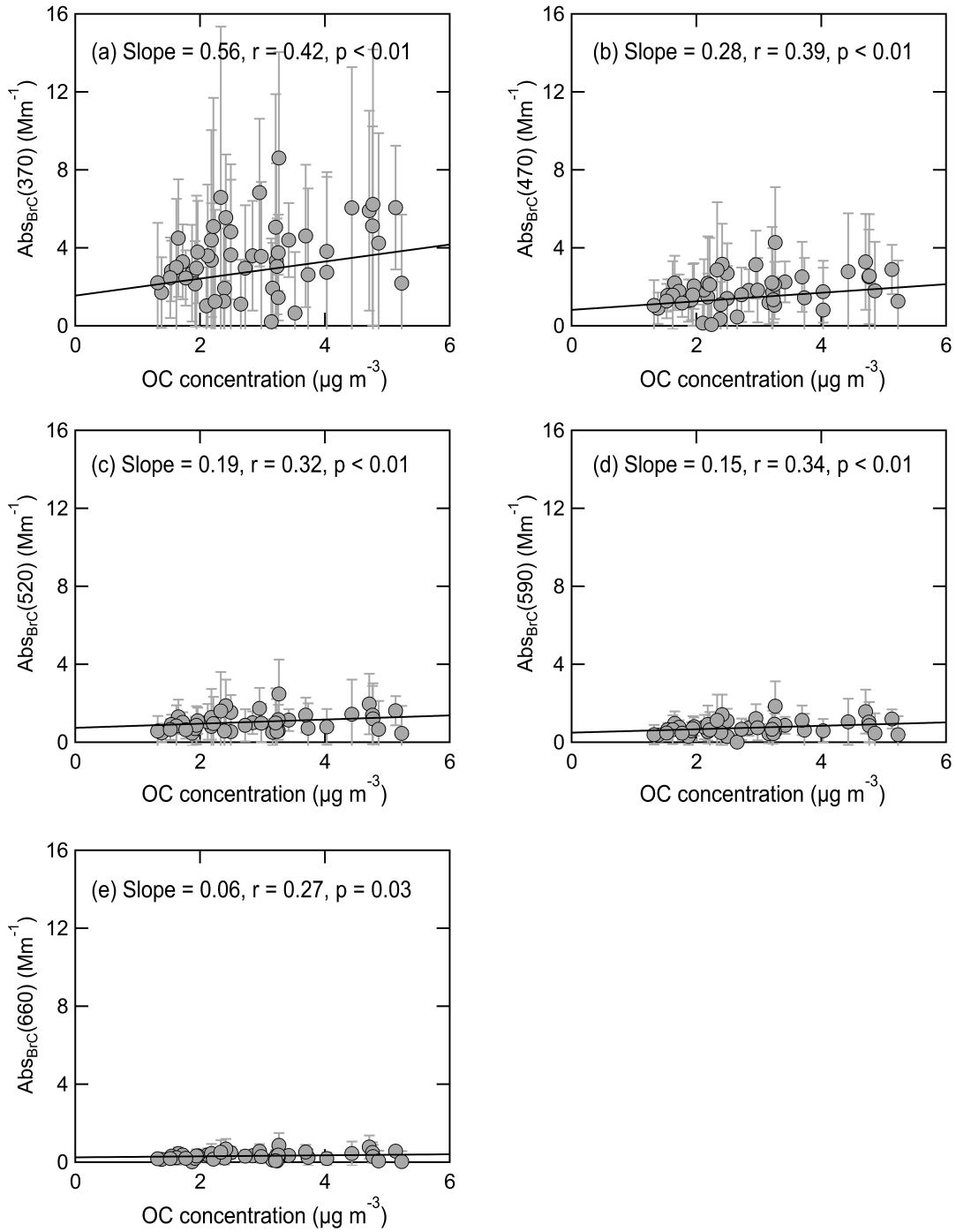

Figure S6. Scatter plots of light absorption of brown carbon at different wavelengths ($Abs_{BrC}(\lambda)$, λ = 370, 470, 520, 590, and 660 nm) versus mass concentration of organic carbon (OC). The black lines are the linear regression. The vertical error bars represent one standard deviation of $Abs_{BrC}(\lambda)$.

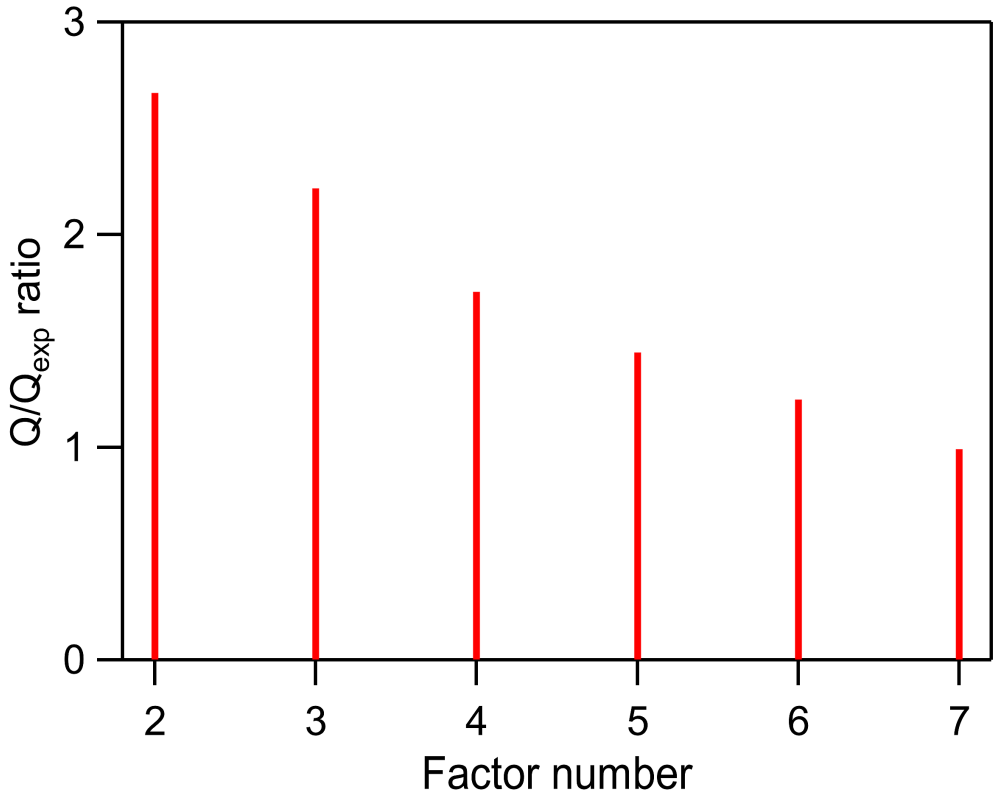

Figure S7. The Q/Q_{exp} ratio as a function of factor number.

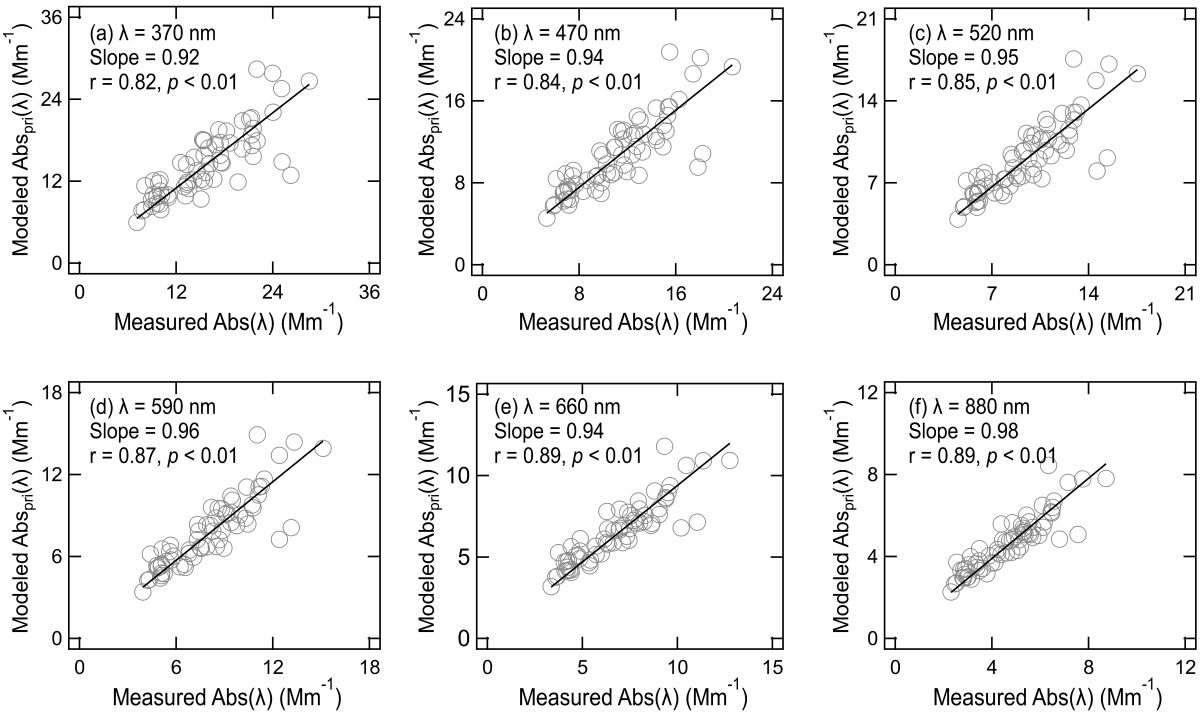

Figure S8. Scatter plots of primary aerosol light absorption ($Abs_{pri}(\lambda)$, λ = 370, 470, 520, 550, 660, or 880 nm) simulated with a positive matrix factorization model versus light absorption (Abs(λ)) measured with AE33 aethalometer.